Measurement of Diffusivity and Solubility of Olefins in Polypropylene by Gas Chromatography

ANDREA SLIEPCEVICH,[1] GIUSEPPE STORTI,[2] MASSIMO MORBIDELLI[2]

[1] Politecnico di Milano, Dipartimento di Chimica Fisica Applicata Via Mancinelli 7, 20131 Milano, Italy

[2] ETH Zürich, Chemical Engineering Department/LTC, Universitätstrasse 6, CH-8092 Zürich, Switzerland

Received 14 September 1999; accepted 4 December 1999

ABSTRACT: The classical gas chromatographic technique is applied to measure the solubility and diffusivity of ethylene and propylene in polypropylene. The polymer particles were used as supplied by the producers to pack the chromatographic columns. This allows a direct measurement of the interested properties in a particle with the same morphology obtained at the reactor outlet. Moreover, the apparatus was adapted to carry out measurements at pressures and temperatures close to those typical of the reaction conditions. The measured values of solubility and diffusivity compare favorably with those predicted by literature relationships for semicrystalline polymeric matrices. Moreover, the estimated diffusivities indicate the diffusion in the polymer microparticles as the rate determining step and a diffusive characteristic length comparable with the particle diameter, i.e., larger than expected in the frame of a multigrain particle schematization. © 2000 John Wiley & Sons, Inc. J Appl Polym Sci 78: 464–473, 2000

Key words: catalytic polymerization; solubility; diffusivity; polyolefins; gas chromatography

INTRODUCTION

Gas phase catalytic polymerization processes are relevant in the production of polyolefins. Due to the very high specific polymerization rates achieved with the last catalyst generations, the understanding of mass and heat transport resistances becomes crucial to process simulation and control. When modeling these processes, the knowledge of the particle morphology and of the involved physicochemical properties is very important. In this work, we develop a technique for measuring two of such properties: solubility and diffusivity of the monomers in a polymer particle under nonreacting conditions.

The technique we discuss here is based on the classical solid–gas chromatography. The columns were packed with the original polymer particles, without any pretreatment except for sieving, which has been used to narrow the size distribution of the packing material. This technique has been extensively used in the past to study heat transport, axial diffusion, adsorption kinetics, and intraparticle diffusivity and porosity (cf. ref. 1). With reference to polymers, almost all previous applications considered a supported (solid or liquid) polymer layer, and used either packed or capillary columns (cf. ref. 2). In this work, we instead packed the column directly with polymer particles as they left the reactor, thus without inducing changes of morphology of either the particle or the polymer. In this respect, this approach

Correspondence to: M. Morbidelli.

Contract grant sponsor: EEC; contract grant number: BE-3022.

Journal of Applied Polymer Science, Vol. 78, 464–473 (2000)

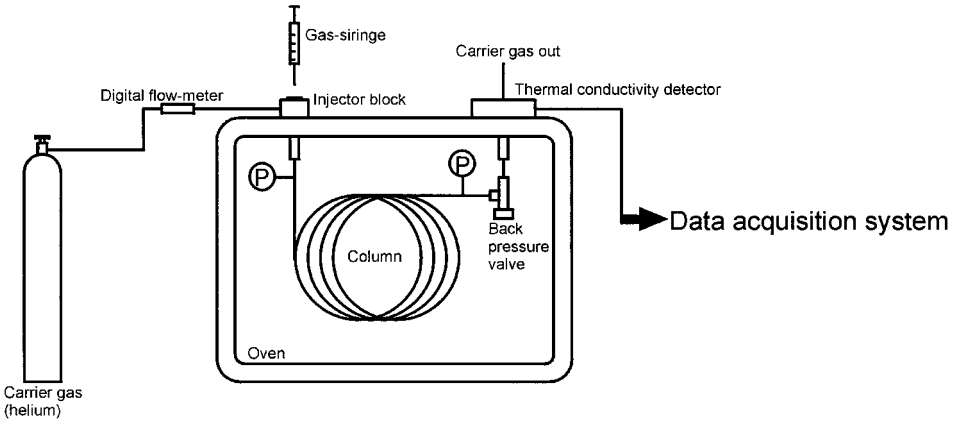

Figure 1 Scheme of the experimental apparatus.

is completely equivalent to that used by Webb et al.[1] for measuring ethylene transport under nascent, reacting conditions, i.e., during the initial reaction stage, with the important differences that here no reaction is taking place and the particle morphology is the final one.

The theoretical approach used to analyze the experimental data is based on the classical equations of linear chromatography (cf. 3). In particular, the moments of the eluted peaks are evaluated to relate the interested quantities (i.e., solubility and diffusivity) to retention time and variance. This theoretical frame is well established, and corrections for extracolumn effects and pressure drop in the column are available. The assumption of linear chromatography was easily fulfilled in all experiments carried out, due to the low absorptivity typically exhibited by olefins in polyolefins.

In the following, we first describe the experimental apparatus and the materials. Then, the equations used to evaluate monomer solubility and diffusivity from the measured eluted peaks are shown. A description of the procedure used to correct the measured quantities for external effects is presented, together with an example of a typical run. Finally, the obtained results are discussed. A comparison with the results of available predictive relationships is made and the rate-determining diffusive step is identified by comparing measurements at different particle sizes and pressures.

EXPERIMENTAL APPARATUS AND MATERIALS

The main features of the experimental apparatus are schematically shown in Figure 1. A gas chromatographic unit HP6890 (indicated as GC in the following), equipped with digital flow control (flow accuracy $\pm 1\%$) and pressure transducer at column inlet, was modified to work up to 7 bar of pressure in the column. A back pressure valve (Nupro R3A Series) and a digital pressure transducer were installed at the outlet of the chromatographic column to set pressure at the desired value and measure pressure drop in the column, respectively. A thermal conductivity detector and a personal computer equipped with a data acquisition system were used to detect and evaluate the solute concentration in the carrier gas (He) leaving the column. This detector was chosen because of its sensitivity to inert species such as nitrogen. The column was fitted to the GC oven where temperature is controlled to ± 0.1°C. The pulse of the component under examination was fed to the GC through the injector port by a 1 cm^3 syringe for gases.

The chromatographic columns were packed using different powders of commercial polypropylene supplied by two different companies, exhibiting the characteristics summarized in Table I.

Both polymers were received fully characterized in terms of density, volume fraction of crystalline polymer ϕ_c, and intraparticle porosity ratio ϵ_p.

Table I Characteristics of the Polymeric Packings at Room Temperature

Polymer	ρ_p (g cm^{-3})	ϕ_c (cm^3 cm^{-3})	ϵ_p
Polypropylene	0.899	0.52	0.12–0.16
Polypropylene	0.901	0.50	0.15–0.19

Table II Characteristics of the Packed Columns

			ϵ^*		
Column	L (cm)	M_p (g)	APP	GC	d_p (μm)
A	540	48.0	0.49	0.46	700–800
B	206	16.1	0.45	0.43	400–500
C	293	26.6	0.40	0.39	200–300
D	103	8.9	0.42	0.42	100–200

Density ρ_p, was measured by picnometry, and the obtained value is in good agreement with that estimated by the following equation:

$$\rho_p = \rho_c\phi_c + \rho_a(1 - \phi_c) \quad (1)$$

where the value of ϕ_c is taken from Table I, while for the density of crystalline ρ_c and amorphous polymer ρ_a, literature values have been used.[4] The fraction of crystalline polymer ϕ_c, has been measured by differential scanning calorimetry. The evaluation of particle porosity ϵ_p, was performed using a simple gravimetric measurement after filling particle pores with a poor solvent (diethyleneglycol[5]). It is worth noting that using Hg porosimetry, much lower values of ϵ_p are obtained (3–4 times smaller), probably due to changes in the volumetric properties of the amorphous part of the polymer induced by the high operating pressures typical of this technique.

Two different particle sizes for each polymer type were used to fill four chromatographic columns whose main characteristics are summarized in Table II. The internal diameter of all columns was equal to 0.45 cm. To produce a column packing with narrow particle size distribution, all polymers were sieved and the size uniformity of the resulting packing was checked by scanning electron microscopy. While the sieving procedure was successful for columns A and B (Figs. 2 and 3), a significant amount of fines was retained in both columns C and D (Figs. 4 and 5), due to electrostatic adhesion of the smaller particles to the sieving apparatus. It was estimated that about 50% of the polymer (on a particle number basis) was well below the target size, thus resulting in a broad/bimodal size distribution. In the same figures (2–5), the different surface morphology of the two polymers is also evident, apparently less "open" in the first (A and B) than in the second case. The microscopic morphology of both polymers as obtained by scanning electron microscopy is shown in Figures 6–9. Even though the photographs correspond to the particle sur-

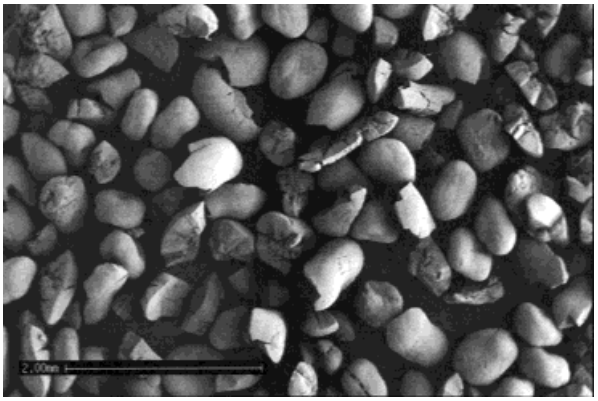

Figure 3 SEM photographs of polymer packing of column B. Magnification = ×20.

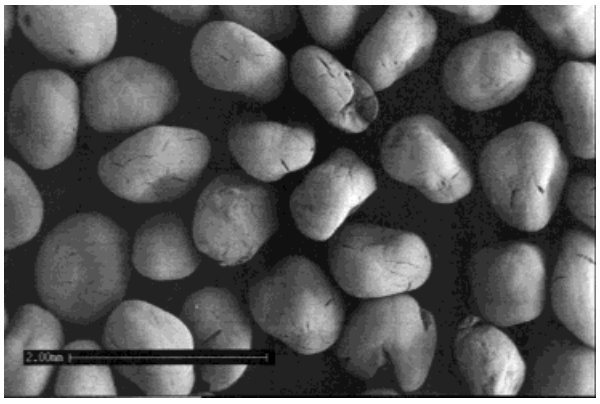

Figure 2 SEM photographs of polymer packing of column A. Magnification = ×20.

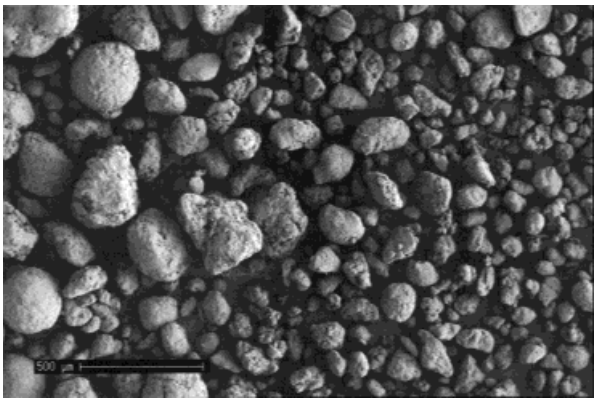

Figure 4 SEM photographs of polymer packing of column C. Magnification = ×50.

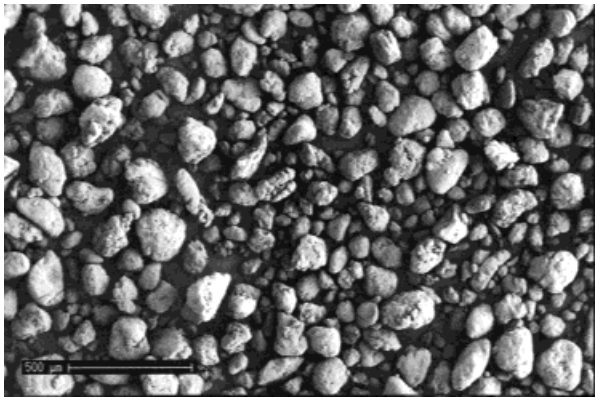

Figure 5 SEM photographs of polymer packing of column D. Magnification = ×50.

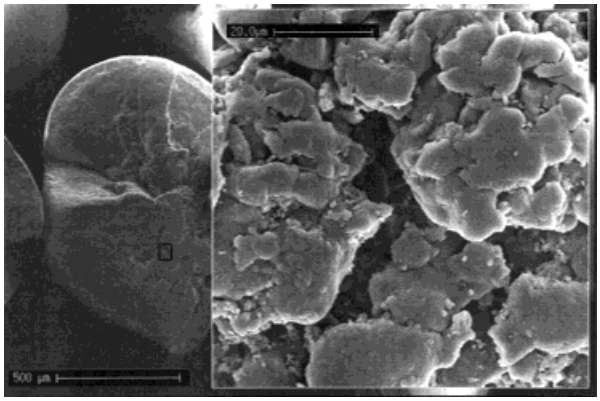

Figure 7 SEM photographs of polymer packing of column B. Magnification = ×50 and ×1000.

face, the "compactness" of the polymer phase is quite apparent. In the case of the first polypropylene in Table I, a cluster-type microstructure can be probably recognized but the microparticles appear very close one to the other thus resulting in a sort of continuous matrix. The same conclusion is even more true in the case of the second polypropylene of Table I, where the microparticles cannot be even roughly identified. In conclusion, the polymer domains appear to be much broader than those expected in the classical multigrain morphology usually considered when modeling reaction kinetics (particles assimilated to clusters of spherical, independent polymer microparticles, cf. ref. 6).

All columns were packed under vacuum and continuous mechanical vibration. The particle diameter is always below one tenth of the column diameter with the exception of column A. This should explain the slightly larger value of the overall void ratio ϵ^* of this column with respect to those estimated in the remaining three cases. Note that this quantity, defined as

$$\epsilon^* = \epsilon + (1 - \epsilon)\epsilon_p \tag{2}$$

accounts for the overall void volume inside the column, both external (ϵ) and internal (ϵ_p) to the polymer particles. The values reported in Table II were measured in two different ways. In the first case (column labeled APP in the table), polymer mass M_p, column volume V_c, and polymer density were combined to give

$$\epsilon^* = 1 - \frac{M_p}{\rho_p V_c} \tag{3}$$

In the second case (column labeled GC in the table), the values were obtained directly through the chromatographic technique by injecting a

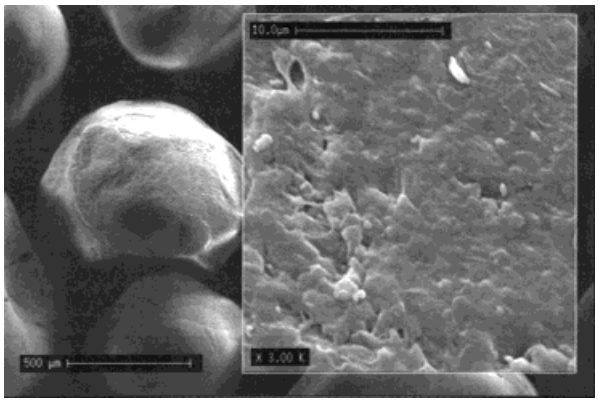

Figure 6 SEM photographs of polymer packing of column A. Magnification = ×50 and ×3000.

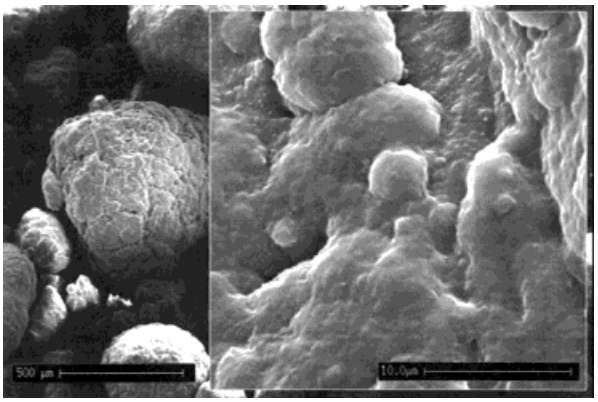

Figure 8 SEM photographs of polymer packing of column C. Magnification = ×50 and ×3000.

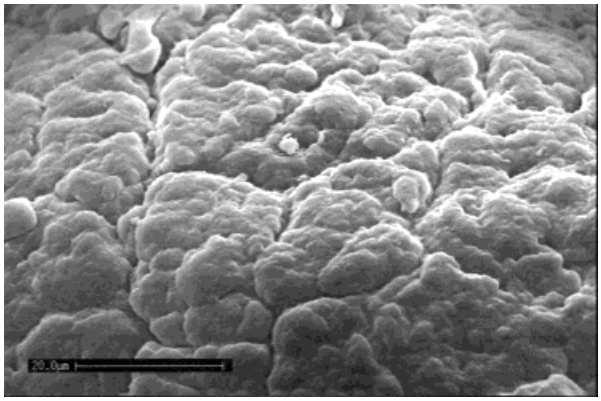

Figure 9 SEM photographs of polymer packing of column D. Magnification = ×2000.

pulse of inert compound, as described in the section Data Reduction. The two sets of values are indeed in good agreement and the numerical values obtained by GC were used in all subsequent calculations.

Finally, note that different column lengths were used, ranging from more than 5 m for column A to about 1 m for column D. These lengths were adjusted as a function of the adopted particle size, thus using shorter columns for smaller particle sizes so as to reduce the pressure drop in the column.

DATA REDUCTION

Basic Equations

The measurements have been performed following the classical elution mode and the results analyzed in the frame of the linear chromatography theory, using the method of moments (cf. ref. 3). Accordingly, the experimental values of retention time $\bar{t}$ and variance σ^2 of the eluted concentration peak are expressed in terms of moments as follows:

$$\bar{t}_{\text{exp}} = \frac{\mu_1}{\mu_0} \tag{4}$$

$$\sigma^2_{\text{exp}} = \frac{\mu_2}{\mu_0} - \frac{\mu_1^2}{\mu_0^2} \tag{5}$$

where μ_i indicates the ith order moment of the concentration peak $C(t)$, defined as

$$\mu_i = \int_0^\infty C(t) t^i \, dt \tag{6}$$

Retention time and peak variance at the column outlet are related to both physicochemical properties of the polymer–monomer system under examination and operating conditions. If a bimodal morphology is considered (spherical polymer microparticles in spherical macroparticles with constant porosity), the following equations apply:

$$\text{retention time} \quad \bar{t} = \frac{L}{v}\left(1 + \frac{1-\epsilon}{\epsilon} K\right) = \frac{L}{u}\left[\epsilon^* + (1-\epsilon^*)K_c\right] \tag{7}$$

where v and u indicate interstitial and superficial carrier velocity, respectively, and K is an overall capacity ratio of the particle, defined as $\epsilon_p + (1 - \epsilon_p)K_c$, with K_c the partition coefficient of the monomer between polymer and gas phase q/C.

$$\text{variance} \quad \sigma^2 = \frac{2L\mathcal{D}_L}{v^3}\left(1 + \frac{1-\epsilon}{\epsilon} K\right)^2 + \frac{2L}{v}\frac{1-\epsilon}{\epsilon} K^2 t_m \tag{8}$$

where $\mathcal{D}_L$ is the axial diffusion coefficient and t_m indicates a characteristic time of intraparticle diffusion, defined as

$$t_m = t_f + t_p + t_c = \frac{d_p}{6k_f} + \frac{d_p^2}{60\mathcal{D}_p} + \frac{d_c^2}{60\mathcal{D}_c}\frac{K - \epsilon_p}{K^2} \tag{9}$$

The three terms in the right-hand side represent the characteristic times for the mass transport in the external fluid film t_f, in the particle pores t_p, and inside the polymer microparticles t_c. The diameters of macro and microparticles are indicated by d_p and d_c, respectively. The k_f indicates the transport coefficient in the fluid film, and $\mathcal{D}_p$ and $\mathcal{D}_c$ are the diffusion coefficients in pore and polymer, respectively. The pore diffusivity is equal to the molecular diffusivity of the monomer reduced by porosity, ϵ_p, and tortuosity factor τ, according to the relationship $\mathcal{D}_p = \mathcal{D}_m \epsilon_p / \tau$.

The two parameters $\bar{t}$ and σ^2 are usually combined into the single quantity HETP, height equivalent to a theoretical plate. This is defined as follows:

$$\mathrm{HETP} = \frac{\sigma^2 L}{\bar{t}^2} \tag{10}$$

and the corresponding expression, known as van Deemter equation,[7] is readily obtained combining eqs. (7) and (8). When plotted as a function of the carrier flow rate, the HETP curve typically exhibits a minimum value, and approaches a linear behavior at large flow rates. The slope of the linear part of the curve is directly related to the characteristic time of diffusion t_m. Therefore, all measurements were carried out at large flow rates to emphasize the role of the intraparticle diffusion resistances.

Corrections for Extracolumn Effects

Under the assumption of linear chromatography conditions, the additional retention and dispersion due to injector, detector, valves, and any other extracolumn part of the unit can be assumed to superimpose to those actually due to the chromatographic column. Then, the following expressions for apparent or experimental values of these quantities apply:

$$\bar{t}_{\mathrm{exp}} = \bar{t}_{\mathrm{col}} + \bar{t}_{\mathrm{ext}} \tag{11}$$

$$\sigma^2_{\mathrm{exp}} = \sigma^2_{\mathrm{col}} + \sigma^2_{\mathrm{ext}} \tag{12}$$

where subscripts "col" and "ext" refer to column and all components of the unit but the column, respectively. The evaluation of these correction factors, $\bar{t}_{\mathrm{ext}}$ and σ^2_{ext}, was performed by elution experiments of an inert compound (air) using columns of different length as bypass. In all cases, the pressure drop through the unit with the bypass was extremely small and the corresponding corrections (applied when the polymer packed columns were used, as detailed in the next subsection) were neglected.

In the case of retention time, an empty short tube with volume 3.8 cm^3 was used. The measured retention times resulted in a net dead volume (i.e., after correction for the void volume of the bypass column) of 2.4 cm^3. On the other hand, the values of σ^2_{exp} evaluated at $P = 4$ atm and $T = 80$°C are shown in Table III as a function of the carrier flow rate. In this case, two columns such as those used for the chromatographic experiments but packed by glass microspheres ($d_p = 75$ μm) and with length 24 and 100 cm, respectively, were installed as bypass. Very similar values

Table III Corrections for Dispersion due to Extracolumn Effects (P = 4 atm; T = 80°C)

Carrier Flow Rate ($\mathrm{Ncm}^3\ \mathrm{min}^{-1}$)	σ^2_{exp} (min^2)	
	L = 24 cm	L = 100 cm
8	0.1334	0.1385
10	0.0767	0.0781
20	0.0125	0.0136
30	0.0046	0.0048
40	0.0022	0.0024

were measured in both cases. This indicates that these dispersions are essentially due to the external part of the unit and that it could be assumed $\sigma^2_{\mathrm{ext}} \simeq \sigma^2_{\mathrm{exp}}$. The negligible contribution of the packed bypass columns was also verified by estimating the corresponding axial mixing coefficient using a predictive relationship from the literature.[8]

Corrections for Pressure Drop

The values of both retention time and dispersion of the column are affected by pressure drop in the column. Since eqs. (7) and (8) apply to isobaric conditions, the experimental values were further corrected to account for the measured pressure drop. The approach proposed by Pazdernik and Schneider[9] was adopted. Accordingly, the following equations were used:

$$\bar{t}_{\mathrm{col}} = \bar{t} f_1 \tag{13}$$

$$\sigma^2_{\mathrm{col}} = \frac{2L\mathcal{D}_L}{v^3}\left(1 + \frac{1-\epsilon}{\epsilon}K\right)^2 f_2 + \frac{2L}{v}\frac{1-\epsilon}{\epsilon} \times K^2\left(\frac{d_p}{6k_f} f_2 + \frac{d_p^2}{60\epsilon_p \mathcal{D}_p} f_2 + \frac{d_c^2}{60\mathcal{D}_c}\frac{K-\epsilon_p}{K^2} f_1\right) \tag{14}$$

where the factors f_j are defined as

$$f_j = \frac{2}{j+2}\frac{(\gamma+1)^{j/2+1} - 1}{\gamma}$$

$$\gamma = \left(\frac{P_{\mathrm{in}}}{P_{\mathrm{out}}}\right)^2 - 1 \tag{15}$$

with P_{in} and P_{out} the inlet and outlet pressure of the column, respectively. Note that this correction results in a nonlinear behavior of HETP as a function of the carrier flow rate when significant pressure drops are present. Therefore, a close lin-

earity of HETP data with velocity provides an indirect experimental check of the negligible relevance of pressure drop.

While the single correction factor f_1 is required for retention time, two different factors, f_1 and f_2, are needed for the peak variance. However, these factors approach one the other at low pressure drops and the use of the following simplified formula:

$$\sigma^2_{col} = \sigma^2 f_1 \tag{16}$$

has been suggested at $\gamma \leq 0.5$.[10] Since the pressure drops typically found in the experiments are well below this value ($0.02 \leq \gamma \leq 0.3$), this simplified equation was used to estimate the isobaric value of the peak dispersion.

Finally, it should be noted that, for both extracolumn as well as pressure drop effects, it was always found that the corresponding corrections were always small, affecting the final results by no more than few percents of the uncorrected values.

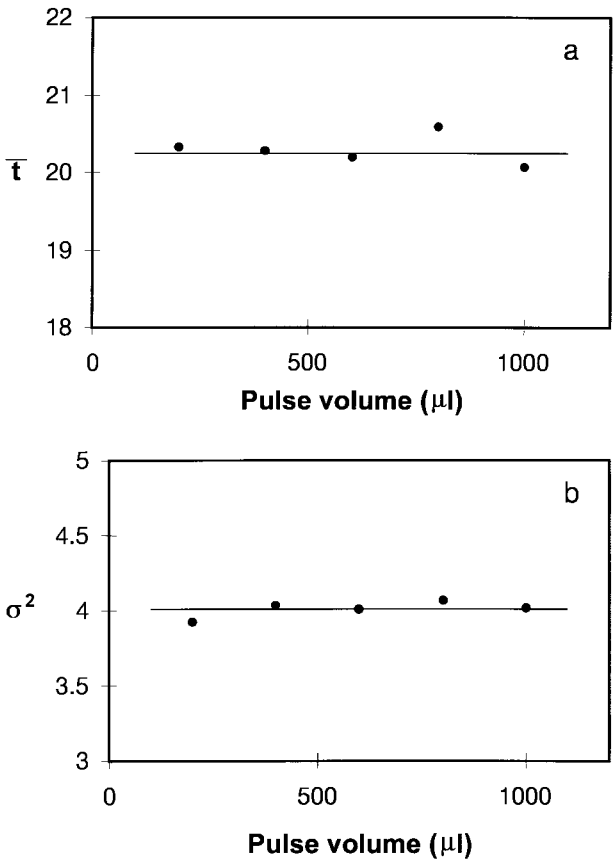

Figure 10 Retention time (a) and peak variance (b) as a function of the injected pulse volume. Column A, ethylene, $T = 80°C$, $P = 6$ atm, flow rate = 15 N cm^3 min^{-1}.

Table IV Typical Set of Experimental Results[a]

Carrier Flow Rate (Ncm^3 min^{-1})	$\bar{t}$ (min)	σ^2_{ext} (min^2)	K_c	HETP (cm)
4	15.19	4.25	0.30	3.89
6	10.42	2.38	0.31	4.63
8	8.01	1.68	0.33	5.51
10	6.50	1.28	0.34	6.38
20	3.36	0.62	0.36	11.68
30	2.28	0.41	0.37	16.42
40	1.74	0.31	0.37	21.23

[a] Column B, ethylene, $T = 80°C$, $P = 6$ atm.

Check of the Linear Conditions

As mentioned above, the analysis so far performed applies only under the assumption of linear chromatography, i.e., linear absorption equilibrium of the monomer in the polymer. To check the reliability of this assumption, preliminary experiments were performed for each column at constant flow rate using pulses of the monomer at constant concentration and increasing volume. In the case of linear chromatography, the measured retention time $\bar{t}$ and peak dispersion σ^2 should be independent of the pulse volume (cf. 3). As an example, the results obtained for column A using ethylene are shown in Figure 10(a) and (b). The expected independence of the obtained result from the volume pulse is well confirmed and the reliability of the assumption thus proved.

A Typical Experimental Run

Finally, the results of a typical experiment (Column B, ethylene, $T = 80°C$, $P = 4$ atm), selected as representative of all measurements performed in this work, are discussed. The values of retention time and peak variance, corrected for extracolumn effects and pressure drop, are reported in Table IV as a function of the carrier flow rate. Note that each value represents the average of a series of three repeated measurements. In the same table the estimated values of K_c and HETP are also reported and the last quantity is plotted as a function of carrier flow rate in Figure 11. Since relatively large values of velocity were examined, a linear behavior is clearly evidenced, thus confirming the reliability of the correction

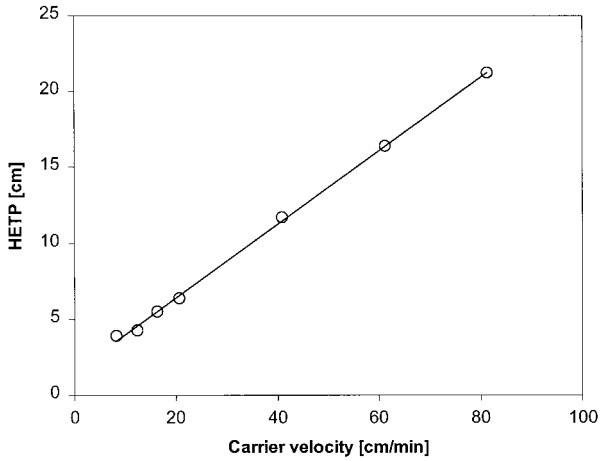

Figure 11 Height equivalent to a theoretical plate, HETP, as a function of carrier velocity. Column B, ethylene, $T = 80°C$, $P = 6$ atm.

applied to account for the effect of pressure drop in the column. As mentioned above, the slope of this straight line is directly related to the characteristic time of diffusion t_m.

RESULTS AND DISCUSSION

The results of all experiments carried out with the four columns of Table II and using ethylene and propylene as monomers are summarized in Table V. In all cases the operating temperature was 80°C. Note that column A, packed with the particles of the largest available size, was used at a single pressure (6 atm), while different pressure values (4–7 atm) were examined for columns B–D.

Solubility Results

The estimated K_c values indicate a practically constant value for each monomer, 0.36 for ethylene and 1.23 for propylene. These values were found at all pressures and for both polypropylenes. The independence of pressure is a further check that a linear equilibrium law applies, as it was expected due to the very low monomer concentrations typically found in chromatographic measurements, well below the limit of validity of the Henry's law. In fact, according to Stern et al.,[11] the monomer partial pressure P^* at which the equilibrium value deviates from linearity by 5% can be estimated through the following equation:

$$\log \frac{P^*}{P_c} = 3.025 - 3.50 \frac{T}{T_c} \tag{17}$$

where P_c and T_c indicate the critical pressure and temperature of the monomer. This equation gives $P^* = 83$ and 12 atm for ethylene and propylene, respectively, which are much larger than the partial pressure of both components in the column, whose maximum total pressure was 7 atm.

The measured K_c values were compared with those predicted by literature a priori relationships. In particular, the solubility of small molecules in the amorphous fraction of rubbery semicrystalline polymers (T_g of polypropylene is about 253 K, well below the operating temperature) can be estimated using two different expressions: (1) the relationship by Stern et al.[11]:

$$\log K = -2.38 + 1.08 \left(\frac{T_c}{T}\right)^2 \tag{18}$$

where the Henry's constant K (mol L^{-1} atm^{-1}) is related to the partition coefficient K_c used in eq. (7) by the following expression:

$$K_c = KRT(1 - \phi_c) \tag{19}$$

and (2) the equation by Michaels and Bixler[12]:

$$S = S_0 \exp\left(-\frac{\Delta H}{RT}\right) \tag{20}$$

Table V Summary of the Experimental Results for Ethylene and Propylene at $T = 80°C$

		Ethylene		Propylene	
Column	P (atm)	K_c	t_m (s)	K_c	t_m (s)
A	6	1.49	45.4	0.45	91.2
B	4	1.23	16.8	0.36	26.6
	5	1.22	17.4	0.35	26.9
	6	1.21	16.6	0.35	26.0
	7	1.24	17.0	0.38	25.1
C	4	1.19	10.6	0.35	11.6
	5	1.24	10.8	0.37	10.6
	6	1.32	10.0	0.39	7.7
	7	1.30	11.1	0.37	11.0
D	4	1.18	7.5	0.34	8.6
	5	1.20	7.3	0.35	9.4
	6	1.23	7.1	0.36	8.5
	7	1.23	6.9	0.35	8.6

where the preexponential factor, S_0, and the activation energy ΔH are evaluated as

$$\log S_0 = -5.5 - 0.005\,\frac{\epsilon}{k} \pm 0.8$$

$$\frac{\Delta H}{R} = 1000 - 10\,\frac{\epsilon}{k} \pm 500 \qquad \text{(K)} \quad (21)$$

The solubility S (cm^3_{STD} cm^{-3} Pa^{-1}) is related to K_c as follows:

$$K_c = S\,\frac{P_{STD}}{T_{STD}}\,T(1 - \phi_c) \qquad (22)$$

where the subscript STD indicates standard conditions, i.e., $P = 1$ atm and $T = 273$ K.

The comparison between predicted and experimental values is shown in Table VI. In all calculations, an average value of the crystalline volume fraction $\phi_c = 0.50$ was used (cf. Table I). The measured K_c values are inside the range of the predicted values for both the monomers, and provide a check of the accuracy of these a priori estimation methods.

Diffusivity Results

The values of the characteristic diffusive time t_m reported in Table V result from the summation of three different diffusive steps: through the external film around the particle, in the macropores and in the polymer matrix, as indicated by eq. (9). Using the relationship by Wakao and Funazkri[8] to evaluate the mass transport coefficient k_f as a function of the flow rate, it is found that the first resistance is always negligible, being the estimated values of t_f at least two orders of magnitude smaller than the experimental values of t_m. Therefore, the measured time values will be discussed in terms of the two intraparticle steps t_p and t_c.

Table VI Comparison Between Measured and Predicted Values of Solubility K_c, and Diffusivity $\mathcal{D}_c$

	Ethylene	Propylene
Solubility, K_c		
Experimental	0.36	1.23
Eq. (19)	0.30	0.87
Eq. (22)	0.54	1.86
Diffusivity, $\mathcal{D}_c$ (cm^2 s^{-1})		
Experimental	$0.6–2.2 \times 10^{-6}$	$0.3–2.0 \times 10^{-6}$
Eq. (27)	0.58×10^{-6}	0.18×10^{-6}

Table VII Values of Diffusivity in Polymer $\mathcal{D}_c$ Estimated Using Eq. (25)

		$\mathcal{D}_c$ (cm^2 s^{-1})	
Column	d_p (μm)	Ethylene	Propylene
A	750	2.2×10^{-6}	2.0×10^{-6}
B	450	2.1×10^{-6}	1.5×10^{-6}
C	250	1.4×10^{-6}	0.4×10^{-6}
D	150	0.6×10^{-6}	0.3×10^{-6}

In order to identify the transport limiting step, the following limiting expressions of t_m are considered, obtained assuming one or the other diffusive step as rate determining:

Diffusion in macropores:

$$t_m = \frac{d_p^2 \tau}{60 \epsilon_p \mathcal{D}_m} \quad \propto d_p^2,\ P^1 \qquad (23)$$

Diffusion in polymer:

$$t_m = \frac{d_c^2}{60\mathcal{D}_c}\,\frac{K - \epsilon_p}{K^2} \begin{cases} \propto d_p^0,\ P^0 & \text{if} \quad d_c \ll d_p \quad (24) \\ \propto d_p^2,\ P^0 & \text{if} \quad d_c \simeq d_p \quad (25) \end{cases}$$

By inspection of the t_m values in Table V for a particular column (i.e., particle size), it is readily concluded that these are independent of pressure, thus indicating that the diffusion in polymer is the rate determining step.

To estimate the scale length of the diffusion process in the polymer matrix (i.e., the characteristic size of the polymer domains), the dependence of t_m upon particle size is analyzed. Since the SEM photographs shown in Figures 6–9 indicate a microparticle size comparable with that of the macroparticle, the limiting case corresponding to eq. (25) has been considered (i.e., $d_c = d_p$) and the diffusivity values shown in Table VII were calculated. These values have been compared with those predicted by literature *a priori* relationships. The following relationship reported by van Krevelen[13] for the diffusion coefficient (cm^2 s^{-1}) in the amorphous fraction of rubbery semicrystalline polymers was used:

$$\mathcal{D} = \mathcal{D}_0 \exp\left(-\frac{E_D}{RT}\right) \qquad (26)$$

where:

$$\frac{E_D}{R} = \left(\frac{\sigma}{\sigma_{N_2}}\right)^2 1000p \pm 600 \qquad \text{(K)}$$

$$p = 7.5 - 2.5\ 10^{-4}(298 - T_g)^2$$

$$\log \mathcal{D}_0 = \frac{E_D}{R}\ 10^{-3} - 4 \pm 0.4$$

Note that, different from the solubility case, the polymeric matrix plays a role in this equation through the parameter p expressed as a function of the polymer glass transition temperature T_g. From this value, the diffusivity in the semicrystalline polymer $\mathcal{D}_c$ can be readily estimated through the following simple expression:

$$\mathcal{D}_c = \mathcal{D}(1 - \phi_c) \qquad (27)$$

usually applied at very low monomer concentrations, as in the case under examination here.

The values predicted through eq. (27) are shown in Table VI, always assuming a constant average value of $\phi_c = 0.5$. A remarkable agreement between experimental and predicted values is obtained. Moreover, it is worth mentioning that completely different diffusivity values are estimated (10^{-11} cm^2 s^{-1}) when the limiting case corresponding to eq. (24) is applied. This means that the scale length of monomer diffusion inside the polymer is of the order of the diameter of the macroparticle. In other words, the particle morphology of these samples resembles more a porous continuum of polymer than a cluster of segregated microparticles. About the variation of the measured coefficient with the particle size indicated in Table VII, it should be pointed out that a larger range of values is found at least in the case of ethylene when considering columns C and D, probably due to the broader particle size distribution characteristic of the last two columns. In fact, as anticipated in the experimental section, the relevant amount of small particles could reduce the difference of average particle size, thus reducing the difference in terms of diffusion coefficients as estimated through eq. (25). Further measurements using the same polymer but with narrower particle size distribution are in progress to better clarify this point.

CONCLUSIONS

Applications of classical chromatography to measure solubility and diffusivity of monomers in polypropylene particles obtained by gas phase catalytic polymerization were reported. The values measured through this technique compare favorably with those predicted by literature relationships, both in the case of ethylene and propylene. All measurements were carried out using "final" polypropylene particles, i.e., under nonreacting conditions but with the actual morphology they have when leaving the reactor. The results indicate that the rate determining step for monomer diffusion in these particles is in the polymer more than in the macropores of the particle. This can be explained if the diffusive characteristic length is close to the size of the whole particle, thus suggesting a pseudocontinuum polymer phase more than a cluster of segregated microparticles as particle morphology. In conclusion, the results obtained in this work indicate chromatography as a relatively simple and reliable technique for measuring solubility and diffusivity of monomers and polymers with well defined morphologies.

The financial support of EEC (CATAPOL Brite/Euram Project BE-3022) is gratefully acknowledged.

REFERENCES

1. Webb, S. W.; Conner, W. C.; Laurence, R. L. Macromolecules 1989, 22, 2885.
2. von Meien, O. F.; Biscaia, E. C., Jr.; Nobrega, R. AIChE J 1997, 43, 2932.
3. LeVan, M. D.; Carta, G.; Yon, C. M. In Perry's Chemical Engineers' Handbook; Perry, R. H., Green, D. W., Eds.; McGraw-Hill: New York, 1997; Chap 16.
4. Quirk, R. P.; Alsamarraie, M. A. A. In Polymer Handbook; Brandrup, J., Immergut, E. H., Eds.; John Wiley & Sons: New York, 1989; Chap V.
5. Mattioli, V.; Martin, C.; McKenna, T. F. 12 Months Report, BRITE Project BE 3022 (Catapol), Brussels, 1998.
6. Hutchinson, R. A.; Chen, C. M.; Ray, W. H. J Appl Polym Sci 1992, 44, 1389.
7. van Deemter, J. J.; Zuiderweg, F. J.; Klinkenberg, A. Chem Eng Sci 1956, 5, 271.
8. Wakao, N.; Funazkri, T. Chem Eng Sci 1978, 33, 1375.
9. Pazdernik, O.; Schneider, P. J Chromatography 1981, 207, 181.
10. Ruthven, D. M.; Ching, C. B. In Preparative and Production Scale Chromatography; Ganetsos, G., Barker, P. E., Eds.; Marcel Dekker: New York, 1992; Chap 26.
11. Stern, S. A.; Mullhaupt, J. T.; Gareis, P. J. AIChE J 1969, 15, 64.
12. Michaels, A. S.; Bixler, H. J. J Polym Sci 1961, 5, 393.
13. van Krevelen, D. W. Properties of Polymers; Elsevier: New York, 1990; Chap 18.